Real-Time Evaluation of Transceiver Performance with Joint Pre- and Post-Optical Equalization for Passband Narrowing Using 500-Gbps Transmission

Akira Masuda
NTT Network Innovation Laboratries
Nippon Telegraph and Telephone Corporation
Yokosuka, Kanagawa, Japan
ak.masuda@ntt.com

Shuto Yamamoto
NTT Network Innovation Laboratries
Nippon Telegraph and Telephone Corporation
Yokosuka, Kanagawa, Japan
shuto.yamamoto@ntt.com

Hiroki Taniguchi
NTT Network Innovation Laboratries
Nippon Telegraph and Telephone Corporation
Yokosuka, Kanagawa, Japan
hi.taniguchi@ntt.com

Masanori Nakamura
NTT Network Innovation Laboratries
Nippon Telegraph and Telephone Corporation
Yokosuka, Kanagawa, Japan
msnr.nakamura@ntt.com

Yoshiaki Kisaka
NTT Network Innovation Laboratries
Nippon Telegraph and Telephone Corporation
Yokosuka, Kanagawa, Japan
yoshiaki.kisaka@ntt.com

***Abstract*— We propose a transceiver configuration with optical pre- and post-equalization for channel distortion and show that the configuration enhances the performance of 500-Gbps/lambda PDM-32QAM real-time transmission and frequency-offset tolerance under a severe bandwidth limitation.**

Keywords—coherent transceiver, optical equalization, real time transmission, passband narrowing,

I. INTRODUCTION

With the exponential growth in communication traffic, much research has focused on increasing the capacity of optical transmission systems [1–3]. To achieve higher capacity, such as over 40 Tbps, high-density wavelength multiplexing is necessary in addition to increasing the bit rate per carrier by using a high baud rate and high-order modulation [3]. For such a situation, the signal degradation due to the impact of passband narrowing (PBN) that occurs when passing through cascaded reconfigurable optical add-drop multiplexer nodes must be considered [4]. While many methods using digital signal processing (DSP) in transmitters (Txs) and receivers (Rxs) have been proposed for mitigating PBN [5, 6], an optimum signal-design method in an environment where channel distortion occurs was theoretically introduced [7]. Since that method is based on signal processing on the Tx and Rx sides, it can be applied using DSP on the transponder. However, for high-baud-rate signals, the advantages of bandwidth equalization with optical signal processing instead of all-digital equalization (DEQ) have been reported from the viewpoint of the requirements for digital-to-analog converters (DACs), such as effective number of bits and peak-average-to-power ratio [8, 9].

In this paper, we propose a Tx and Rx configuration with joint pre- and post-optical equalization (OEQ) based on a previous study [7] for PBN. With this configuration using a real-time optical transponder we developed, the required optical signal-to-noise power ratio (OSNR) improved by 0.8 dB at a 0.6-dB Q-factor margin from the forward error correction (FEC) threshold of a 500-Gbps 66-Gbaud PDM-32QAM signal with 3-dB optical bandwidth of 65 GHz after two spans of 70-km transmission. When a 3-GHz frequency offset exists, we also experimentally found that the Q-factor margin with our configuration decreases only by less than 0.2 dB while without our configuration it decreases by 0.46 dB.

II. TRANSCEIVER CONFIGURATION WITH JOINT PRE- AND POST-OPTICAL EQUALIZATION FOR CHANNEL DISTORTION

Figures 1(a) and 1(b) show the conventional Tx and Rx configuration and the proposed configuration with joint pre- and post-OEQ. In the proposed configuration, optical equalizers are provided at the output of the IQ modulator (IQM) on the Tx side and the input of the 90° optical hybrid on the Rx side. The optical equalizers jointly compensate for channel distortions such as PBN, on the basis of the method described below. We also explain the optimum signal-design method under conditions in which the signal is distorted in the channel, as shown in a previous study [7]. Figure 2 shows the system model for designing the modulation and demodulation filters. Here, $G_T(f)$ and $G_R(f)$ indicate the filter responses on the Tx and Rx sides, respectively, and $C(f)$ indicates the channel-frequency response. We assume that $C(f)$ known for $|f| \le W$, where W is bandwidth, and that $C(f) = 0$ for $|f| > W$. In this situation, $G_T(f)$ and $G_R(f)$ may be selected to minimize the error probability at the detector. In addition, $G(f)$ must be selected to satisfy the zero inter-symbol-interference condition, and in special cases in which the additive noise at the input to the demodulator is white Gaussian noise, the optimal filters response of $G_T(f)$ and $G_R(f)$ are

$$|G_T(f)| = K_1 \frac{|X_{rc}(f)|^{1/2}}{|C(f)|^{1/2}}, |f| \le W \tag{1}$$

$$|G_R(f)| = K_2 \frac{|X_{rc}(f)|^{1/2}}{|C(f)|^{1/2}}, |f| \le W \tag{2}$$

where X_{rc} is the raised cosine spectrum with an arbitrary roll-off factor, and K_1 and K_2 are the arbitrary scale parameters. Note that $G_R(f)$ is consistent with $G_T(f)$. From the above equations, the SNR is maximized when the filters on the Tx and Rx sides equalize the channel frequency response at a ratio of 50:50. The SNR at the detector in this case is as follows.

$$SNR = \frac{2P_{av}T}{N_0}\left[\int_{-W}^{W} \frac{|X_{rc}(f)|}{|C(f)|} df\right]^2, |f| \le W \tag{3}$$

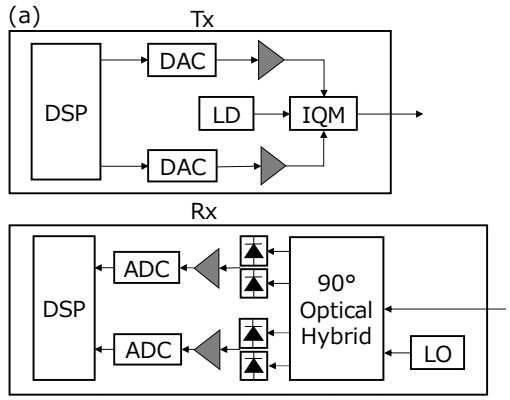

Fig. 1(a). Conventional configuration.

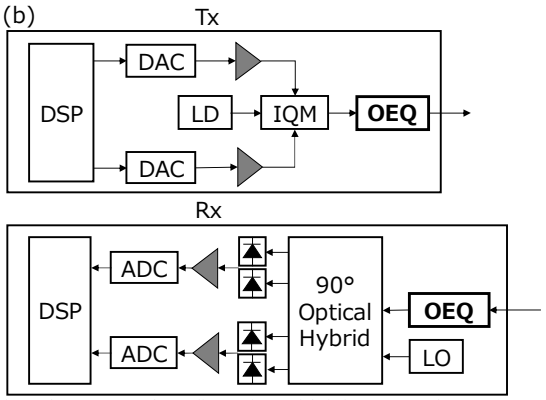

Fig. 1(b). Proposed configuration with joint pre- and post-OEQ.

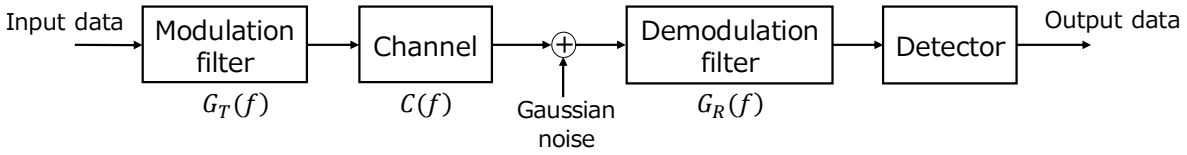

Fig. 2. System model for designing modulation and demodulation filters.

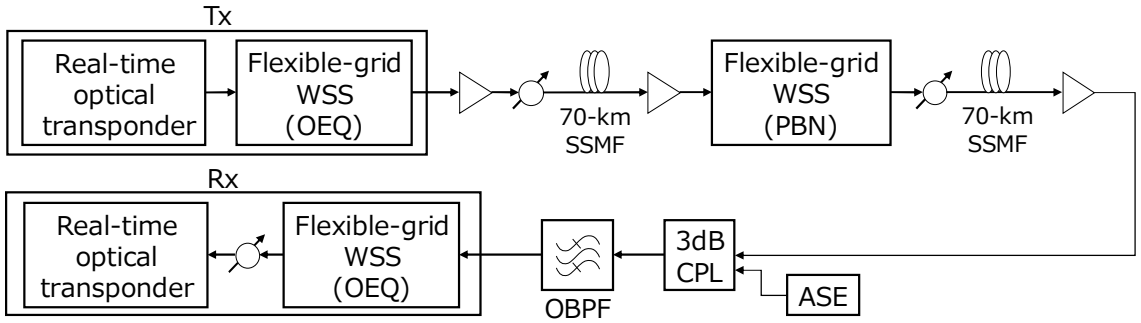

Fig. 3. Experimental setup.

where P_{av} is the average transmitter power, T is symbol period and N_0 is power spectral density of the additive noise.

III. Experimental Setup and Results

Figure 3 shows the experimental setup used to evaluate the performance of the proposed configuration based on the signal design for channels with distortion. In this experiment, a 500-Gbps/lambda 66-Gbaud PDM-32QAM signal was generated using our developed real-time optical transponder. The carrier frequency of the signal was set to 193.8 THz. The optical signal was launched into a straight transmission line consisting of two 70-km spans of standard single-mode fiber (SSMF), three flexible-grid wavelength selective switches (WSSs), and three erbium-doped fiber amplifiers (EDFAs). The 3-dB bandwidth of the center WSS was set to 65 GHz to emulate PBN. The optical signal distortion caused by the center WSS was equalized by the Tx- and Rx-side WSSs. The fiber input power was adjusted to +2 dBm at both spans by using variable optical attenuators (VOAs).

On the Rx side, after post-amplification by an EDFA, the received signal was coupled to amplified spontaneous emission (ASE) at a 3-dB coupler (CPL) and filtered by a 1.2-nm optical bandpass filter (OBPF). The received signal power was adjusted to −7 dBm by using a VOA. The received signal was then coherently detected, equalized, demodulated, and decoded using the optical transponder.

Figure 4(a) shows the relationship between the OSNR and Q-factor margin from the FEC threshold for the 500-Gbps 66-Gbaud PDM-32QAM with and without joint pre- and post-OEQ with no fiber links. For without joint pre- and post-OEQ (i.e., conventional configuration), optical-signal distortion was compensated using the all-Rx DEQ on the transponder. In this experiment, we plotted the results of the various Tx- and Rx-side equalization ratios: Tx:Rx = 50:50 (case 1), 25:75 (case 2), 75:25 (case 3), 100:0 (case 4), and 0:100 (case 5). As shown in this figure, case 1 had a 0.7-dB lower required OSNR to achieve the same Q-factor margin than that without joint pre- and post-OEQ in a low-OSNR region, such as 30 dB. For a higher OSNR region, such as 34 dB, there were no performance differences between case 1 and all-Rx DEQ. This is because the noise enhancement caused by ASE is negligible when PBN is compensated using the all-Rx DEQ. However, performance improvement in the low-OSNR region becomes more important because it is usually based on system performance near the FEC threshold. For all cases of joint pre- and post-OEQ at an OSNR of 30 dB, we confirmed that the post-FEC bit error rate is error free for the 500-Gbps/lambda signal. Figure 4(b) illustrates the experimental results with transmission links consisting of two 70-km spans of SSMF. Even when fiber transmission was executed, performance improvement with our configuration was confirmed. Finally, the Q-factor margin at an OSNR of 30 dB when the transponder frequency was changed from −4 to +3 GHz is shown in Fig. 5. For +3-GHz frequency offset, the Q-factor

margin with our configuration was only reduced by less than 0.2 dB compared with that of no frequency offset, while with the conventional configuration it decreased by 0.46 dB. Frequency offset tolerance for PBN is therefore enhanced by applying the proposed configuration. Figure 6 shows the comparison of optical signal spectrums with joint pre- and post-OEQ varied in accordance with the Tx-to-Rx equalization ratio.

IV. CONCLUSION

We proposed a transmitter and receiver configuration with joint pre- and post-OEQ on the basis of signal design for channel distortion. We experimentally demonstrated the real-time performance of the proposed configuration, and the experimental results indicate that it could improve the required OSNR by 0.8 dB at a 0.6-dB Q-factor margin compared with that of a conventional configuration for 500-Gbps/lambda 66-Gbaud PDM-32QAM 140-km transmission with a 3-dB optical bandwidth of 65 GHz. We also experimentally showed that the frequency-offset tolerance for PBN is enhanced by applying this configuration.

ACKNOWLEDGMENTS

This work was supported by the Ministry of Internal Affairs and Communications (MIC), Research and Development of Innovative Optical Network Technology for a Novel Social Infrastructure (JPMI00316) (Technological Theme I).

REFERENCES

[1] J. Renaudier et al., "First 100-nm Continuous-Band WDM Transmission System with 115Tb/s Transport over 100km Using Novel Ultra-Wideband Semiconductor Optical Amplifiers," European Conference on Optical Communications (ECOC), 2017, Th.PDP.A.3.

[2] J. X. Cai et al., "51.5 Tb/s Capacity over 17,107 km in C+L Bandwidth Using Single Mode Fibers and Nonlinearity Compensation," European Conference on Optical Communications (ECOC), 2017, Th.PDP.A.2.K. Elissa, "Title of paper if known," unpublished.

[3] A. Matsushita et al., "41-Tbps C-Band WDM Transmission With 10-bps/Hz Spectral Efficiency Using 1-Tbps/λ Signals," Journal of Light wave Technology, 2020, Vol.38, No.11.

[4] T. Zami et al., "Growing impact of optical filtering in future WDM networks," Optical Fiber Communications Conference and Exhibition (OFC), 2019, M1A.6.

[5] Q. Hu et al., "3.6-Tbps Duobinary 16-QAM Transmission with Improved Tolerance to Cascaded ROADM Filtering Penalty," European Conference on Optical Communications (ECOC), 2018, Tu3G.2.

[6] J. Pan et al., "Real-Time ROADM Filtering Penalty Characterization and Generalized Precompensation for Flexible Grid Networks," IEEE Photonics Journal, 2017, Vol.9, No.3.

[7] J. Proakis, "Digital Communications", McGraw-Hill Higher Education, 2001.

[8] Z. Zhou et al., "Impact of Analog and Digital Pre-Emphasis on the Signal-to-Noise Ratio of Bandwidth-Limited Optical Transceivers," IEEE Photonics Journal, 2020, Vol.12, No.2.

[9] A. Matsushita et al., "64-GBd PDM-256QAM and 92-GBd PDM-64QAM Signal Generation using Precise-Digital-Calibration aided by Optical-Equalization," Optical Fiber Communications Conference and Exhibition (OFC), 2019, W4b.2.

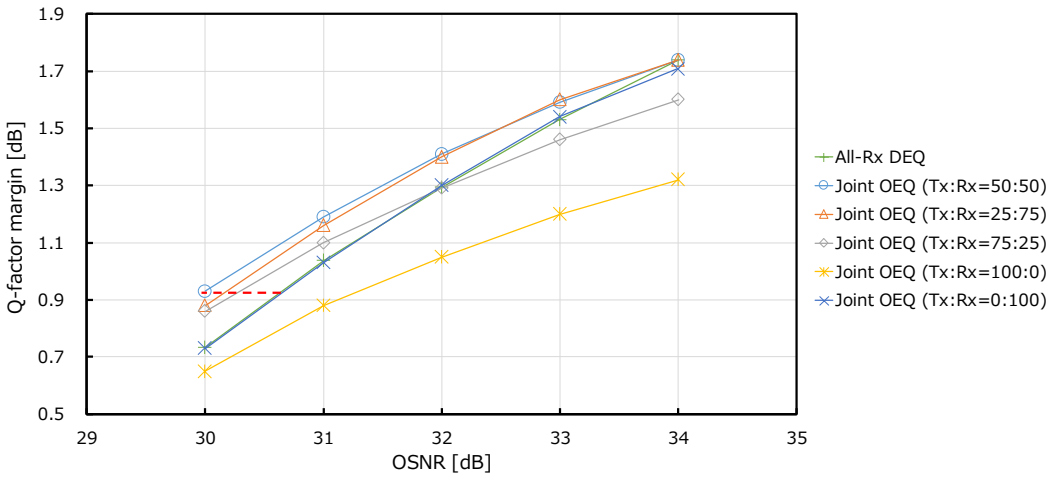

Fig. 4(a). Q-factor margin from FEC threshold without fiber transmission.

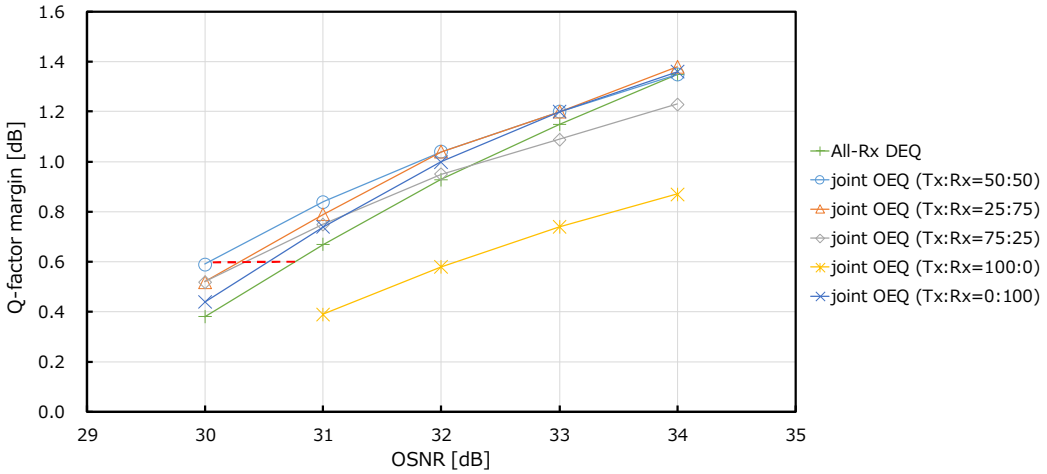

Fig. 4(b). Q-factor margin from FEC threshold with transmission of two spans of 70-km SSMF.

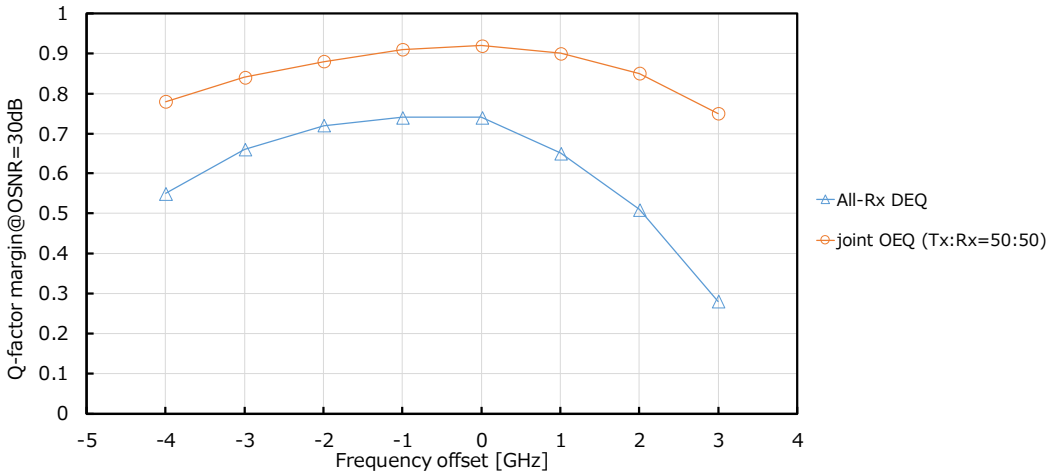

Fig. 5. Comparison of frequency offset tolerances between all-Rx DEQ and joint pre- and post-OEQ at OSNR of 30 dB.

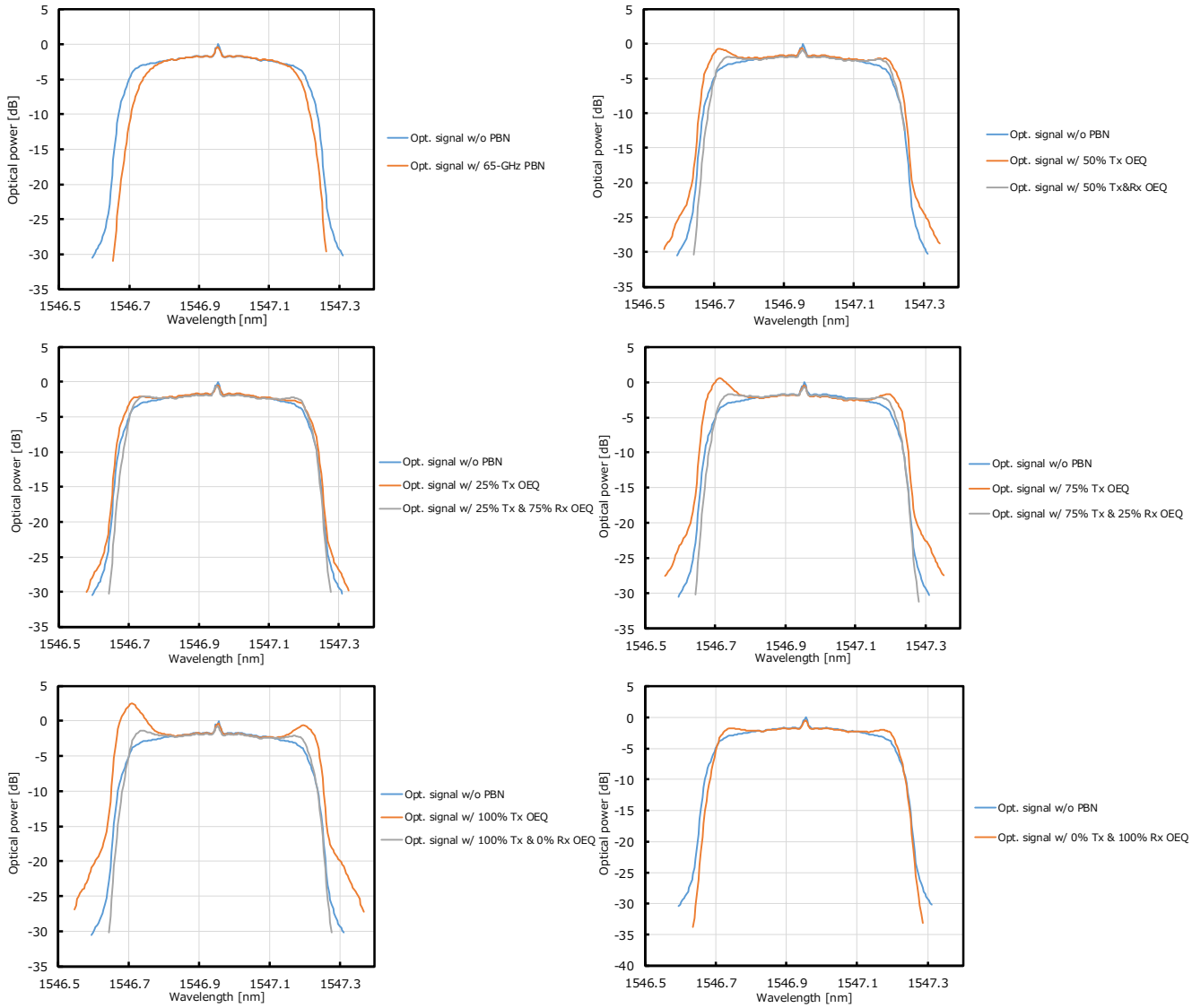

Fig. 6. Comparison of optical spectrums of Tx and Rx sides with joint pre- and post-OEQ.